Published in final edited form as:
Bioorg Med Chem Lett. 2012 March 1; 22(5): 2015–2019. doi:10.1016/j.bmcl.2012.01.028.

Structure-activity relationship study of beta-carboline derivatives as haspin kinase inhibitors

Gregory D. Cuny[a,b,*], **Natalia P. Ulyanova**[c], **Debasis Patnaik**[c], **Ji-Feng Liu**[d], **Xiangjie Lin**[d], **Ken Auerbach**[a,b], **Soumya S. Ray**[e], **Jun Xian**[b], **Marcie A. Glicksman**[a,b], **Ross L. Stein**[a,b], and **Jonathan M.G. Higgins**[c]

[a]Laboratory for Drug Discovery in Neurodegeneration, Brigham & Women's Hospital and Harvard Medical School, 65 Landsdowne Street, Cambridge, MA 02139, USA

[b]Partners Center for Drug Discovery, Brigham & Women's Hospital and Harvard Medical School, 65 Landsdowne Street, Cambridge, MA 02139, USA

[c]Division of Rheumatology, Immunology and Allergy, Department of Medicine, Brigham & Women's Hospital and Harvard Medical School, Smith Building, 5th floor, 1 Jimmy Fund Way, Boston, MA 02115, USA

[d]Aberjona Laboratories, Inc., 100 Cummings Center, Suite 242-F, Beverly, MA 01915, USA

[e]Center for Neurologic Diseases, Department of Neurology, Brigham & Women's Hospital and Harvard Medical School, 65 Landsdowne Street, Cambridge, MA 02139, USA

Abstract

Haspin is a serine/threonine kinase that phosphorylates Thr-3 of histone H3 in mitosis that has emerged as a possible cancer therapeutic target. High throughput screening of approximately 140,000 compounds identified the beta-carbolines harmine and harmol as moderately potent haspin kinase inhibitors. Based on information obtained from a structure-activity relationship study previously conducted for an acridine series of haspin inhibitors in conjunction with *in silico* docking using a recently disclosed crystal structure of the kinase, harmine analogs were designed that resulted in significantly increased haspin kinase inhibitory potency. The harmine derivatives also demonstrated less activity towards DYRK2 compared to the acridine series. *In vitro* mouse liver microsome stability and kinase profiling of a representative member of the harmine series (**42**, LDN-211898) are also presented.

The serine/threonine kinase haspin (Haploid Germ Cell-Specific Nuclear Protein Kinase, also known as Germ Cell Specific Gene-2; Gsg2)[1] functions in mitosis, where it phosphorylates histone H3 at Thr-3 (H3T3ph).[2] During mitosis, this phosphorylation generates a binding site on H3 for Survivin and thereby positions the Chromosome Passenger Complex at centromeres to regulate chromosome segregation,[3, 4] and it also displaces proteins such as TFIID that normally bind to H3 through methylated Lys-4.[5]

---

*To whom correspondence should be addressed: Phone: 617-768-8640, Fax: 617-768-8606, gcuny@rics.bwh.harvard.edu.

Supplementary data

Supplementary data associated with this article can be found, in the online version, at ().

Depletion of haspin by RNA interference, or microinjection of H3T3ph antibodies, causes chromosome alignment defects and failure of normal mitosis.[2, 3, 6]

Human haspin has ATP-binding and catalytic sites structurally similar to other members of the eukaryotic protein kinase (ePK) superfamily with several notable exceptions. For example, the highly conserved DFG motif involved in ATP binding and the APE motif involved in stabilizing the C-terminal lobe among ePKs are altered or absent and the activation loop region is substantially rearranged in haspin compared to other ePKs.[7, 8]

Haspin kinase inhibitors are expected to be useful probes for elucidating the cellular roles of this protein and may have therapeutic utility in treating cancer. A recently described small molecule, CHR-6494 (**1**), that inhibits haspin displayed anti-tumor activity in a mouse xenograft model.[9] Also, 5-iodotubercidin (**2**) has been reported as an effective haspin kinase inhibitor.[7, 10]

We previously utilized a time-resolved fluorescence resonance energy transfer (TR-FRET) high throughput screening (HTS) assay to identify the acridine derivative **3** (LDN-192960) as another potent haspin inhibitor (Figure 1; IC_{50} = 0.010 μM).[11, 12] This assay has now also been used to discover the beta-carbolines harmine, **4**, and harmol, **5**, as moderately potent haspin inhibitors with IC_{50} values of 0.59 and 0.77 μM, respectively. Harmine has previously been identified as an inhibitor of DYRK family kinases, with IC_{50} values between 0.03 and 0.35 μM reported for DYRK1A, and approximately 50-fold lower potency toward DYRK2.[13] Herein, we describe the design, synthesis and improved potency of the beta-carboline series for haspin inhibition utilizing the structure-activity relationships previously determined for the acridine series[12] combined with *in silico* docking using a recently disclosed crystal structure of the kinase.[7] In addition, *in vitro* mouse liver microsome stability and kinase profiling of a representative beta-carboline analog are presented.

A crystal structure of haspin bound to AMP was used for docking calculation.[7, 14] Analysis of this structure revealed key hydrogen bonds between nitrogen atoms of the adenine ring of AMP and protein backbone atoms of residues E606 and G608 (Figure S1).[15] A 12Å docking grid was generated using the AMP center of mass as the point of origin with a single hydrogen bond constraint on the backbone amide of G608. Docking calculations were performed on **3**, which demonstrated that this inhibitor was well accommodated within the binding site and satisfied the hydrogen bonding constraint on G608 (Figure 2). In addition, the inhibitor also made a hydrogen bond with K511, which likely disrupts a key salt bridge between this residue and E535 that is necessary for closure of the ATP-binding cleft enabling kinase activity. A metadynamic simulation sampling the two torsion angles (X^1 and X^2) of the alkylamine as collective variables was also conducted. One low energy conformation was found (Figure S2) that allowed a hydrogen bond between the amine and D611 (Figure 2).

Next, docking calculations were performed on four harmine analogs (**7a** – **b** and **9a** – **b**) that incorporate at two different positions alkylamines similar to that present in **3**. The two derivatives with the alkylamine on the N^9-position (**9a** and **9b**) were well accommodated within the binding site making a hydrogen bond with D687 as well as the hydrogen bonding constraint on G608 (Figure 3B and C). In contrast, compounds **7a** and **7b** resulted in steric hindrance with the region around F607 and G608 and were not well situated within the ATP-binding site, suggesting that they would unlikely be haspin inhibitors. A similar metadynamic simulation for **9a** sampling two torsion angles (X^1 and X^2) of the alkylamine as collective variables found two low energy conformations (Figure 3A). One of these allowed a hydrogen bond between the amine and D611 (Figure 3B), similar to **3**. However,

the second conformation permitted a hydrogen bond between the amine and the backbone carbonyl of I490 in the glycine-rich loop (Figure 3C).

The initial beta-carboline derivatives used in the *in silico* docking experiments were prepared using the procedure outlined in Scheme 1. Harmol, **5**, was *O*-alkylated with N-Boc-protected alkylamines in the presence of cesium carbonate to give **6a** and **6b**. The carbamate protecting group was removed under acidic conditions to give **7a** and **7b**. Harmine, **4**, could be *N*-alkylated. However, phthalimide-protected alkylamines were required and a stronger base (i.e. NaH) was also needed to give **8a** and **8b**. Removal of the protecting group was accomplished using hydrazine hydrate to yield **9a** and **9b**.

Haspin kinase inhibitory activity for the various compounds was assessed using the same assay utilized for the HTS, except in the presence of varying concentrations of test compounds.[11, 15] As anticipated **7a** and **7b** were inactive haspin inhibitors at 10 μM. However, **9a** and **9b** were both active demonstrating IC_{50} values of 0.46 and 0.17 μM, respectively (Table 1).

Based on these results additional beta-carboline analogs were prepared using the general procedure outlined in Scheme 2. Indoles **10** were either directly converted to derivative **11** using $Me_2NCH{=}CHNO_2$ (generated from $MeNO_2$ and $Me_2NCH(OMe)_2$ at 85 °C for 0.5 h) or in a two step procedure (i.e. Vilsmeier-Haak followed by Henry reactions). The alkene and nitro groups were both reduced in the presence of lithium aluminum hydride (LAH) to give **12**. A Pictet-Spengler reaction between **12** and various aldehydes generated **11**. In the case where $R^1 = CF_3$, the hemiacetal $CF_3CHOH(OEt)$ was used. Oxidation of the tetrahydro-beta-carboline with manganese dioxide gave **14**. Finally as previous outlined, alkylation generated **15**, which was de-protected to give **16**.

Several other beta-carboline derivatives were also prepared using the procedures outlined in Scheme 3. Intermediate **17** was de-methylated using HBr in acetic acid to give phenol **18**. This material was converted to triflate **17** and then a methylsulfonamide was introduced utilizing a Pd-catalyzed reaction to yield **20**. Removal of the protecting group gave amine **21**. Likewise, intermediate **16** was converted to the t-butyl ether **22** in the presence of $Me_2NCH(O\text{-}t\text{-}Bu)_2$, which was again de-protected to liberate amine **23**. Intermediate **17** was also de-protected to give **24**, which was converted to the tertiary amine **25** through reductive amination. Finally, intermediate **24** was converted to the secondary amine **27** via the formamide **26**.

The additional compounds prepared were used to further explore the structure-activity relationship of **9b** for haspin inhibition (Table 1). Removal of the methyl at the 1-position (**28**) or replacement with an isopropyl (**29**) were detrimental, where as replacement with an ethyl (**30**) was equivalent. Replacing the methoxy in the 7-position with a hydroxyl (**31**) was tolerated, but a fluorine (**32**), methyl sulfonamide (**33**) or t-butoxy (**34**) were detrimental. Transposition of the methoxy to the 5- or 6-positions (**35** and **36**) resulted in loss of activity, while introduction of the methoxy to the 8-position (**37**) was more tolerated. The 6,7- and 7,8-disubstituted analogs **38** and **39** demonstrated less activity. The primary amine also appeared to be optimal, where the secondary (**40**) and tertiary (**41**) amines were less active. Finally, in order to potentially improve metabolic stability analogs (**42** and **43**) that replace the methyl group in the 1-position with a trifluoromethyl were evaluated. Gratifyingly, **42** displayed an IC_{50} value of 100 nM for inhibiting haspin. This compound was also assessed for *in vitro* metabolic stability in pooled mouse liver microsomes and demonstrated excellent stability with a $t_{1/2}$ of 341 min and a CL_{int} of 3.8 μL/min/mg protein suggesting that this compound may be useful as an in vivo probe.[15, 16]

The beta-carboline series was also evaluated for inhibition of human DYRK2 using a previously described assay.[12] Harmine and harmol gave IC_{50} values for DYRK2 inhibition of 0.69 and 1.5 μM, consistent with previous studies.[13] Introduction of the tethered amine onto the N^9-position substantially reduced the potency for DYRK2 inhibition in all cases examined (Table 1). For example, **42** had an IC_{50} value for DYRK2 of 15 μM and demonstrated 150-fold selectivity for haspin over DYRK2.

Lastly, haspin inhibitor **42** was assessed against a panel of 292 kinases at 10 μM. At this high concentration, the compound inhibited thirteen kinases, in addition to haspin, ≥ 90%.[15, 17] These kinases were CaMK2b, CaMK2d, CDK7-CycH-Mat1, cGK2, CK1d, CLK1, CLK2, DYRK1A, DYRK1B, DYRK3, PASK, PIM1 and PKD3. Interestingly, many of these enzymes belong to the CMGC group of kinases, unlike haspin which is a divergent member of the ePK family.[18] In addition, a comparison of the profiles of **3** and **42** suggested that only six kinases, including haspin, were inhibited by both compounds ≥ 90% at 10 μM (Figure 4).[12] Profiling of additional haspin kinase inhibitors, such as **1** and **2**, may further reduce the number of kinases, besides haspin, which are known to be potently inhibited by all the compounds. In addition, the collective use of **3**, **42** and potentially other haspin inhibitors in cell based assays may allow for more concrete conclusions to be reached with regard to haspin's biological functions.

In conclusion, a structure-activity relationship study of the beta-carbolines **4** and **5**, identified utilizing a recently developed HTS assay for haspin kinase inhibitory activity, was performed guided by insights obtained from a previously optimized compound series[12] combined with *in silico* docking and metadynamic calculations. Increased potency was accomplished by introduction of a tethered primary amine onto the N^9-position of the beta-carboline. Potency was further increased by replacing the methyl at the 1-position with a trifluoromethyl giving **42**. In addition, this analog demonstrated excellent *in vitro* metabolic stability in pooled mouse liver microsomes. Kinase profiling of **42** suggested that it was fairly selective and inhibited only six kinases (≥ 90% at 10 μM), including haspin, in common with the previously identified acridine inhibitor **3**. The beta-carboline haspin inhibitor **42** (LDN-211898) described herein, along with other structurally distinct inhibitors such as **1** – **3** provide valuable molecular probes to study the cellular functions of haspin kinase and may have potential therapeutic utility in treating cancer.

Supplementary Material

Refer to Web version on PubMed Central for supplementary material.

Acknowledgments

The authors thank Partners Healthcare for financial support. This work was also supported in part by NIH grant R01CA122608 and a Leukemia and Lymphoma Society Scholar Award to J.M.G.H.

References and notes

1. (a) Tanaka H, Yoshimura Y, Nishina Y, Nozaki M, Nojima H, Nishimune Y. FEBS Lett. 1994; 355:4. [PubMed: 7957958] (b) Tanaka H, Yoshimura Y, Nozaki M, Yomogida K, Tsuchida J, Tosaka Y, Habu T, Nakanishi T, Okada M, Nojima H, Nishimune Y. J. Biol. Chem. 1999; 274:17049. [PubMed: 10358056]
2. (a) Dai J, Sultan S, Taylor SS, Higgins JMG. Genes Dev. 2005; 19:472. [PubMed: 15681610] (b) Higgins JMG. Chromosoma. 2010; 119:137. [PubMed: 19997740]
3. Wang F, Dai J, Daum JR, Niedzialkowska E, Banerjee B, Stukenberg PT, Gorbsky GJ, Higgins JMG. Science. 2010; 330:231. [PubMed: 20705812]

4. (a) Kelly AE, Ghenoiu C, Xue JZ, Zierhut C, Kimura H, Funabiki H. Science. 2010; 330:235. [PubMed: 20705815] (b) Yamagishi Y, Honda T, Tanno Y, Watanabe Y. Science. 2010; 330:239. [PubMed: 20929775]
5. Varier RA, Outchkourov NS, de Graaf P, van Schaik FMA, Ensing HJL, Wang F, Higgins JMG, Kops GJPL, Timmers HThM. EMBO J. 2010; 29:3967. [PubMed: 20953165]
6. Dai J, Kateneva AV, Higgins JMG. J. Cell Sci. 2009; 122:4168. [PubMed: 19910498]
7. Eswaran J, Patnaik D, Filippakopoulos P, Wang F, Stein RL, Murray JW, Higgins JMG, Knapp S. Proc. Natl Acad. Sci. U.S.A. 2009; 48:20198. [PubMed: 19918057]
8. Villa F, Capasso P, Tortorici M, Forneris F, de Marco A, Mattevi A, Musacchio A. Proc. Natl Acad. Sci. U.S.A. 2009; 48:20204. [PubMed: 19918049]
9. Huertas D, Soler M, Moreto J, Villanueva A, Martinez A, Vidal A, Charlton M, Moffat D, Patel S, McDermott J, Owen J, Brotherton D, Krige D, Cuthill S, Esteller M. Oncogene. 2011
10. Balzano D, Santaguida S, Musacchio A, Villa F. Chem. Biol. 2011; 18:966. [PubMed: 21867912]
11. Patnaik D, Xian J, Glicksman MA, Cuny GD, Stein RL, Higgins JMG. J. Biomol. Screen. 2008; 13:1025. [PubMed: 18978305]
12. Cuny GD, Robin M, Ulyanova NP, Patnaik D, Pique V, Casano G, Liu J-F, Lin X, Xian J, Glicksman MA, Stein RL, Higgins JMG. Bioorg. Med. Chem. Lett. 2010; 20:3491. [PubMed: 20836251]
13. (a) Bain J, Plater L, Elliott M, Shpiro N, Hastie CJ, McLauchlan H, Klevernic I, Arthur JSC, Alessi DR, Cohen P. Biochem J. 2007; 408:297. [PubMed: 17850214] (b) Seifert A, Allan LA, Clarke PR. FEBS J. 2008; 275:6268. [PubMed: 19016842] (c) Göckler N, Jofre G, Papadopoulos C, Soppa U, Tejedor FJ, Becker W. FEBS J. 2009; 276:6324. [PubMed: 19796173] (d) Ogawa Y, Nonaka Y, Goto T, Ohnishi E, Hiramatsu T, Kii I, Yoshida M, Ikura T, Onogi H, Shibuya H, Hosoya T, Ito N, Hagiwara M. Nat. Commun. 2010; 1:86. [PubMed: 20981014]
14. Protein Data Base (PDB) ID: 3DLZ. Docking experiments were conducted using Glide XP *v2.5* from Schrödinger Inc.
15. See supplementary data for details.
16. Baranczewski P, Stańczak A, Sundberg K, Svensson R, Wallin A, Jannson J, Garberg P, Postlind H. Pharmacol. Rep. 2006; 58:453. [PubMed: 16963792]
17. Although the percent inhibition was conducted as a single point, this should reflect relative potency for each kinase. However, dose-response IC_{50} value determinations will ultimately be needed.
18. (a) Higgins JMG. Protein. Sci. 2001; 10:1677. [PubMed: 11468364] (b) Kannan N, Taylor SS, Zhai Y, Venter JC, Manning G. PLoS Biol. 2007; 5:e17. [PubMed: 17355172]

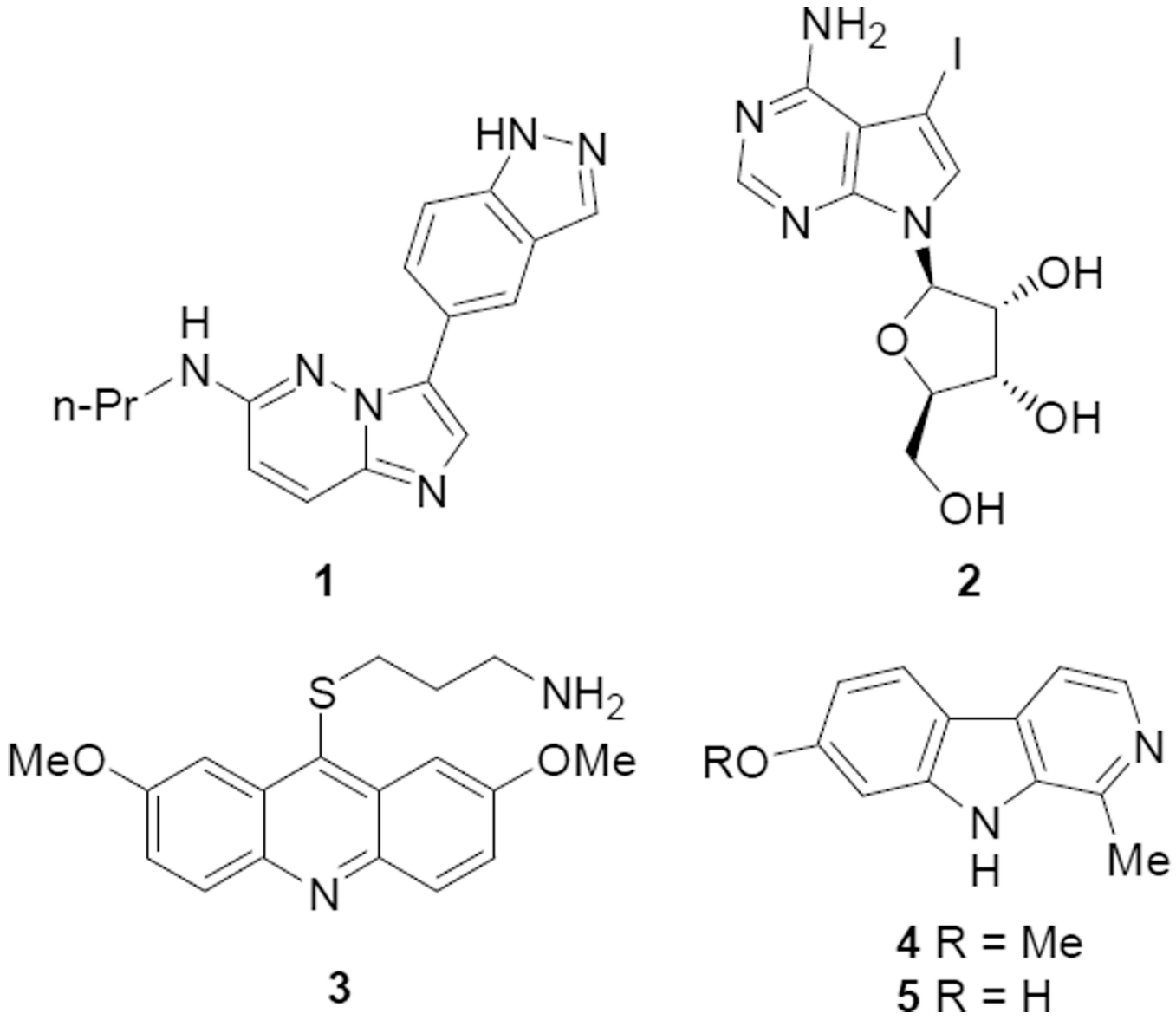

Figure 1.
Haspin inhibitors identified by radiometric, thermal stability shift and TR-FRET HTS assays.

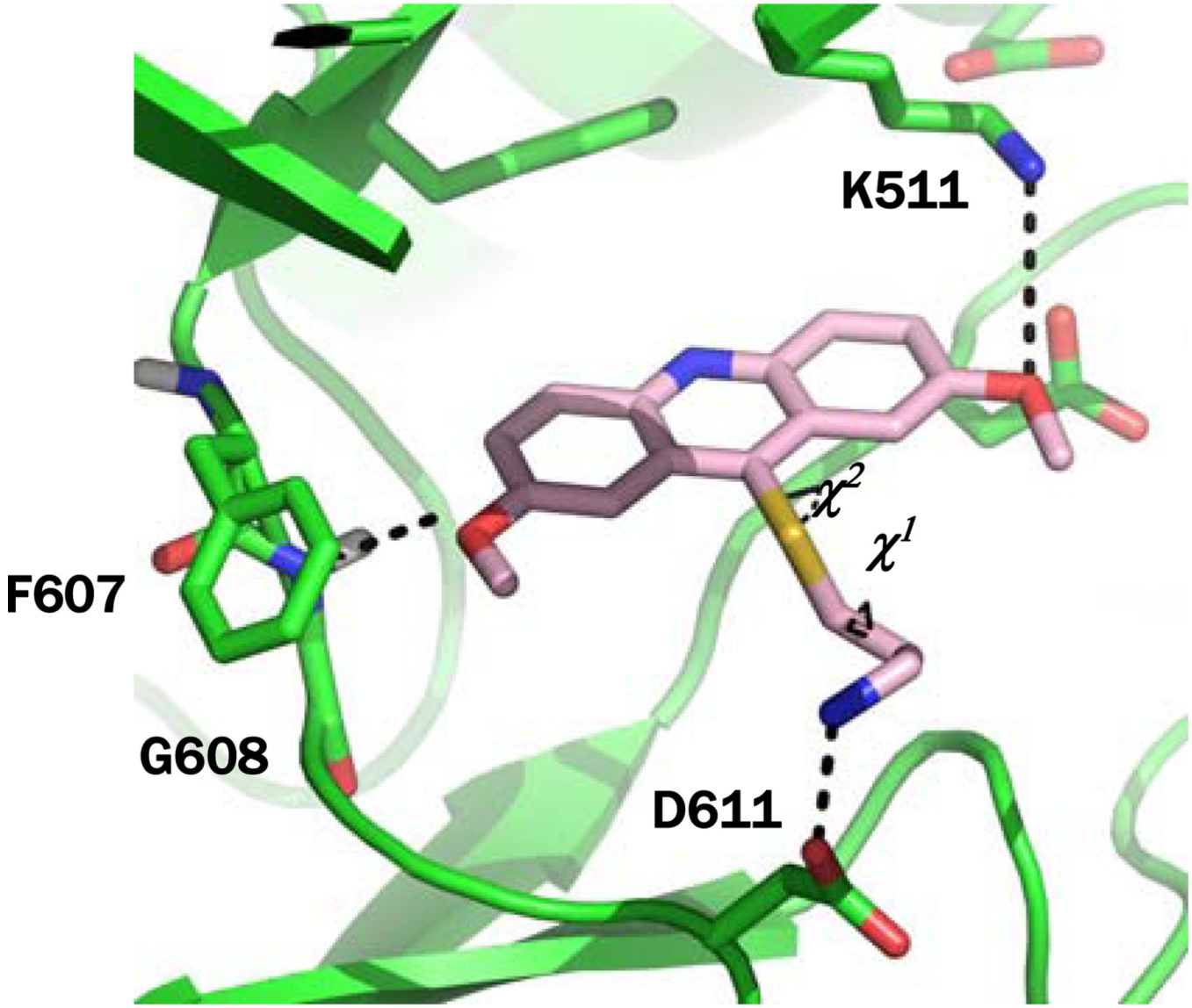

Figure 2.
Molecular docking of **3** at the ATP-binding site of haspin. X^1 and X^2 are the torsion angles that were sampled during the metadynamic calculation.

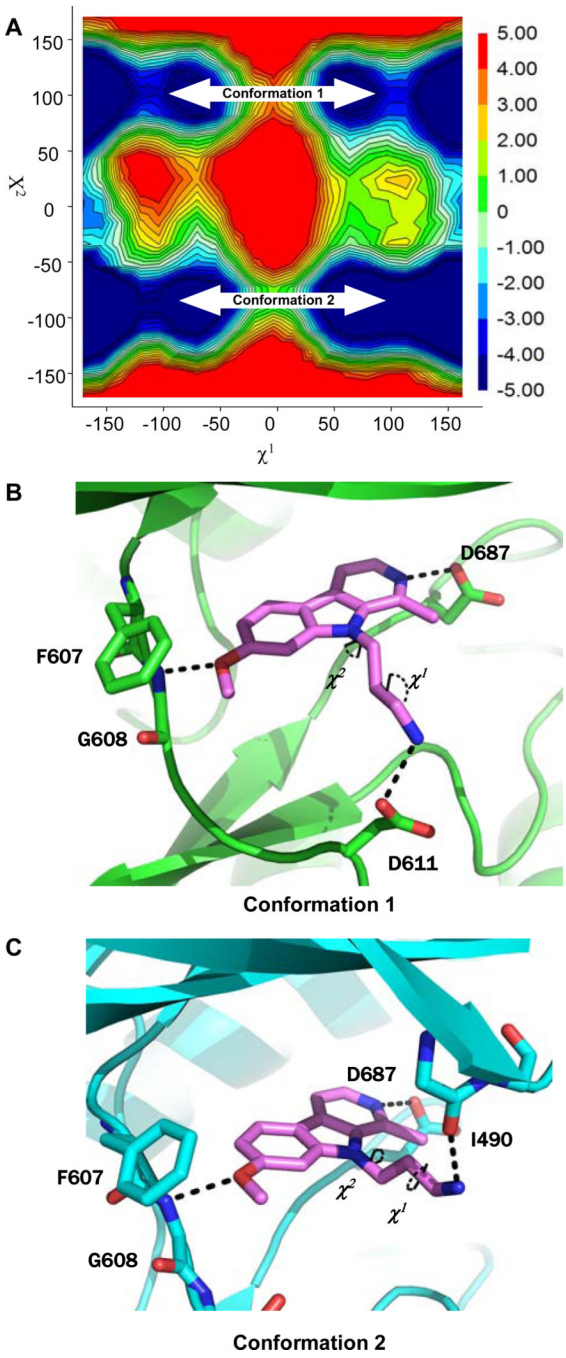

Figure 3.

(A) Free energy surface map from metadynamic calculations sampling two torsion angles (X^1 and X^2) of **9a**. Blue and red represent low and high energy conformations, respectively. (B and C) Docking of **9a** at the ATP-binding site of haspin for the two conformations of the alkylamine side-chain based on metadynamic calculations.

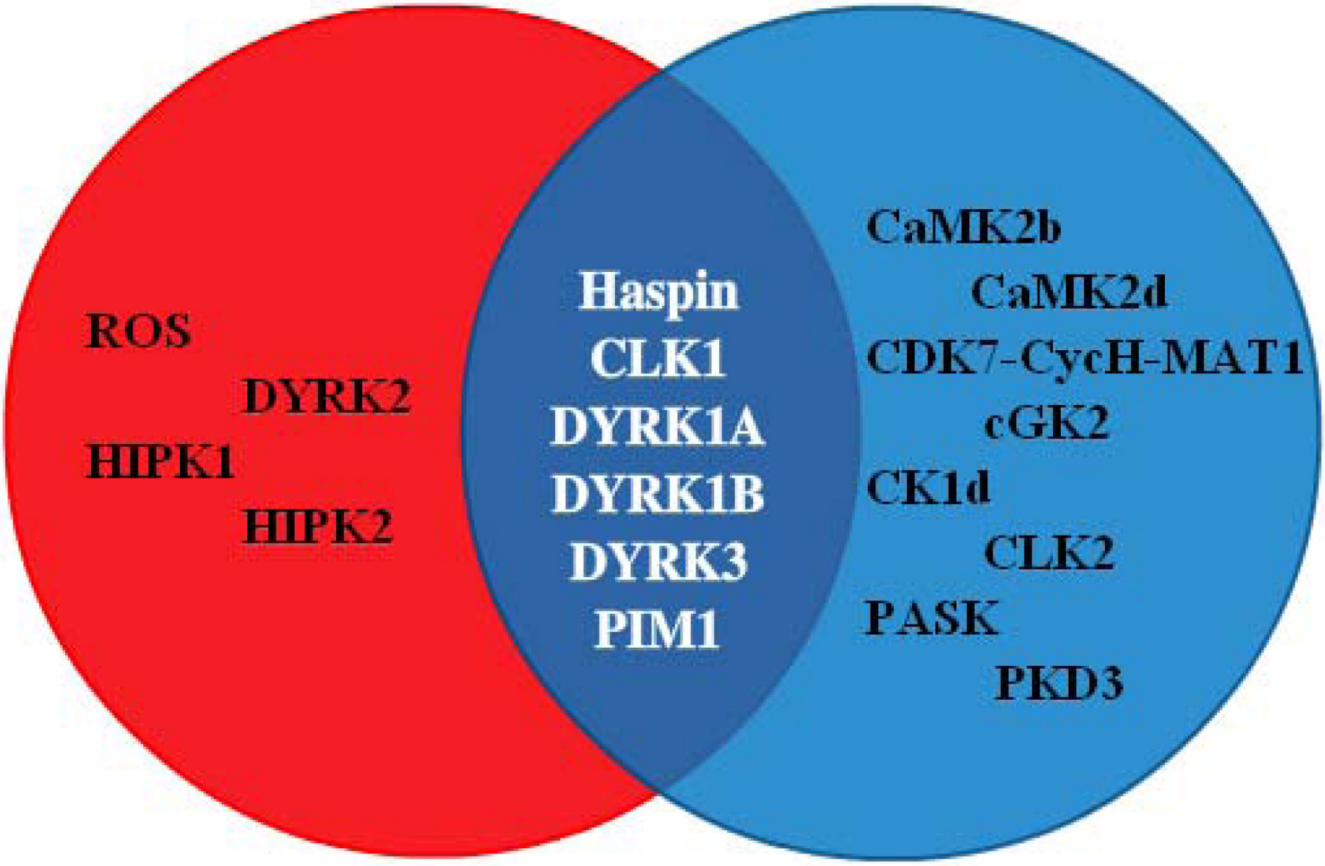

Figure 4.

A Venn diagram highlights kinases selectively inhibited by **3** (red) or **42** (blue) by ≥ 90% at 10 μM. The overlapping region contains only six kinases inhibited by both compounds.

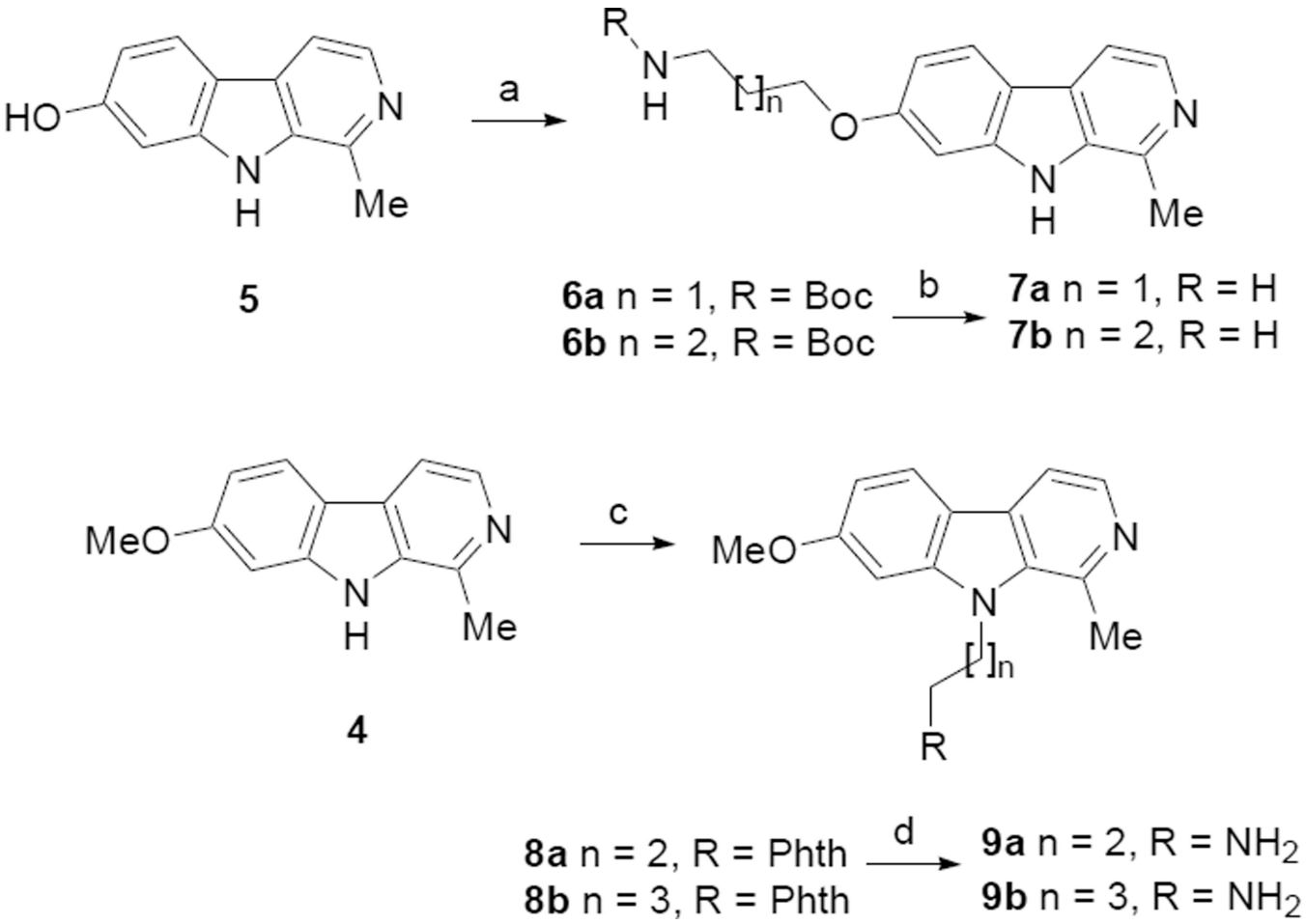

Scheme 1.

Reagents and conditions: (a) $Br(CH_2)_nNHBoc$, Cs_2CO_3, DMF, rt; (b) HCl, MeOH, rt; (c) $Br(CH_2)_nNPhth$, NaH, DMF, rt; (d) $NH_2NH_2 \cdot H_2O$, EtOH, 65 °C. Phth = phthalimide.

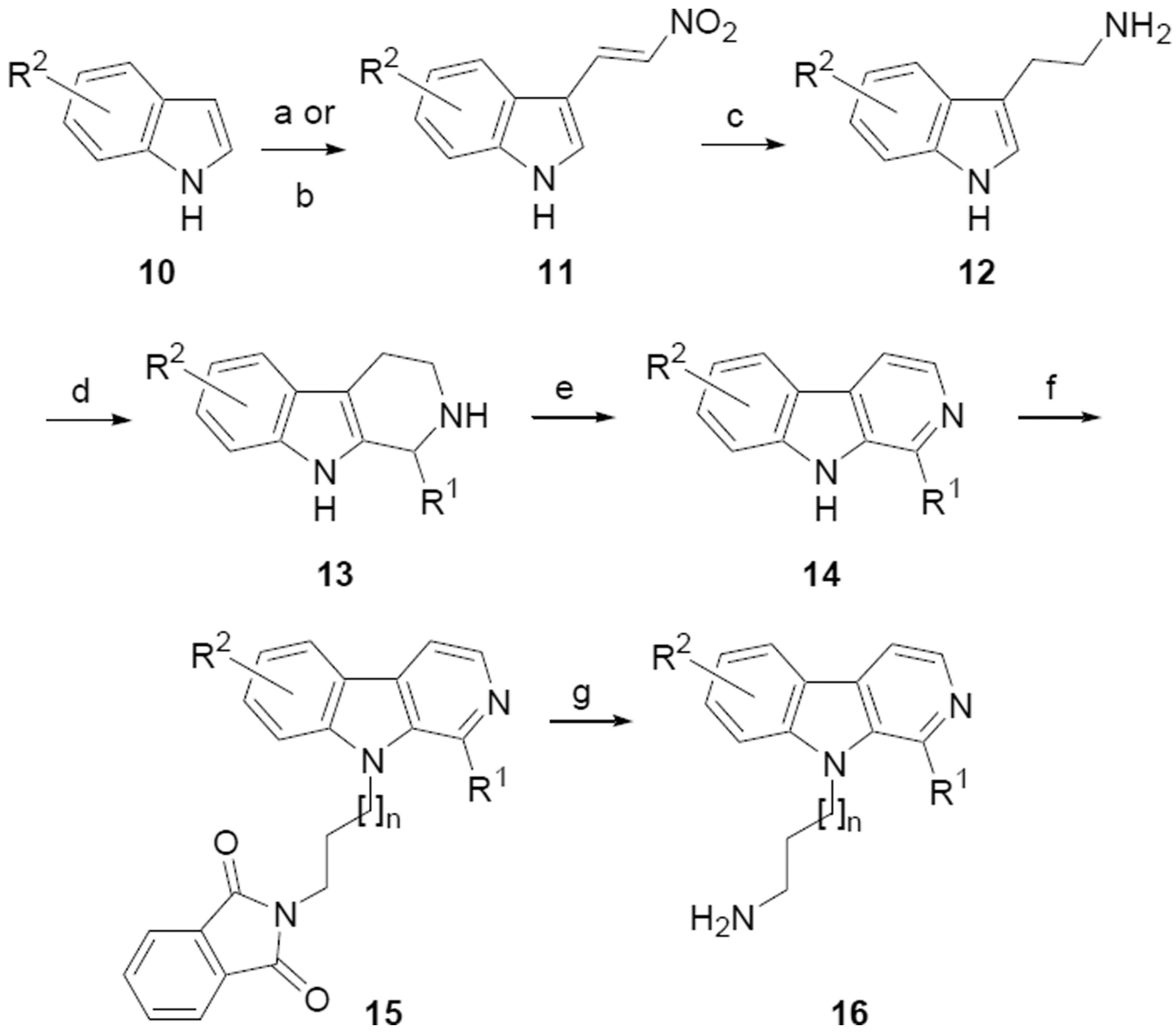

Scheme 2.

(a) $Me_2NCH{=}CHNO_2$, TFA, rt, 30 min; (b) $POCl_3$, DMF, 0 °C to rt then $MeNO_2$, NH_4OAc, 100 °C, 1 h; (c) $LiAlH_4$, THF, rt; (d) R^1CHO or $CF_3CHOH(OEt)$, MeOH, cat. HCl, rt; (e) MnO_2, 5% Pd/C, DMF, microwave (MW), 150 °C; (f) $Br(CH_2)_nNPhth$, NaH, DMF, rt; (g) $NH_2NH_2{\bullet}H_2O$, MeOH, DCM.

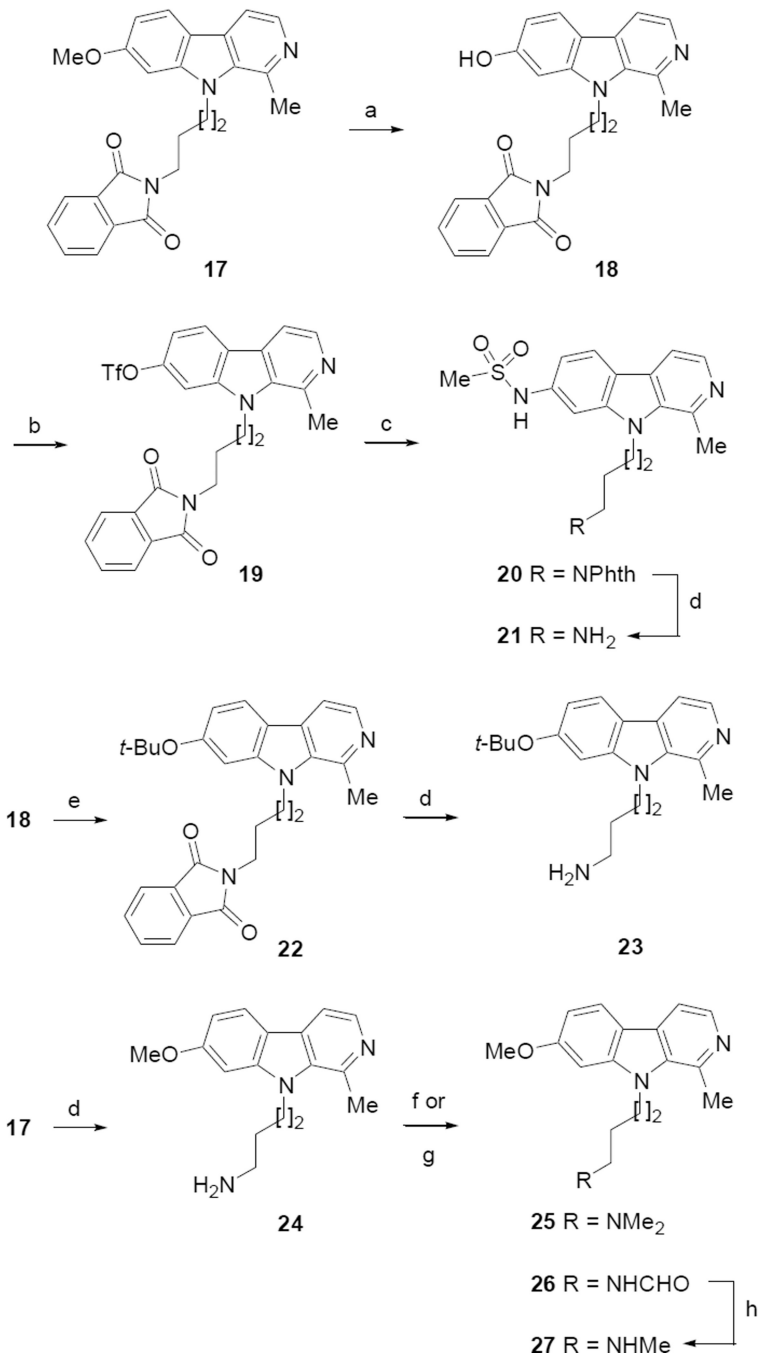

Scheme 3.

(a) HBr, AcOH, MW, 130 °C; (b) Tf_2O, *i*-Pr_2EtN, DCM, 0 °C to rt; (c) $MeSO_2NH_2$, $Pd_2(dba)_3$, xPhOS, K_3PO_4, toluene, 110 °C, 1 h; (d) $NH_2NH_2{\bullet}H_2O$, MeOH, DCM; (e) $Me_2NCH(O\text{-}t\text{-}Bu)_2$, DMF, 120 °C, 1 h; (f) CH_2O, HCO_2H, MW, 150 °C; (g) EtOCHO, MW, 160 °C; (h) $LiAlH_4$, THF, rt.

Table 1

IC_{50}determinations for haspin and DYRK2 inhibition.

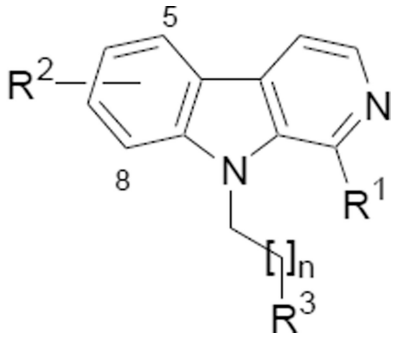

Cmpd	R^1	R^2	R^3	n	IC_{50} (μM)	
					Haspin	DYRK2
9a	Me	7-OMe	NH_2	2	0.46	> 10
9b	Me	7-OMe	NH_2	3	0.17	> 10
28	H	7-OMe	NH_2	3	0.30	> 10
29	*i*-Pr	7-OMe	NH_2	3	0.46	> 10
30	Et	7-OMe	NH_2	3	0.19	> 10
31	Me	7-OH	NH_2	3	0.16	> 10
32	Me	7-F	NH_2	3	0.58	> 10
33	Me	7-$NHSO_2Me$	NH_2	3	0.69	> 10
34	Me	7-O-*t*-Bu	NH_2	3	4.6	> 10
35	Me	5-OMe	NH_2	3	2.7	7.0
36	Me	6-OMe	NH_2	3	2.4	4.9
37	Me	8-OMe	NH_2	3	0.22	> 10
38	Me	6,7-OCH_2O	NH_2	3	0.50	4.8
39	Me	7-OMe, 8-Cl	NH_2	3	0.83	8.0
40	Me	7-OMe	NHMe	3	0.34	> 10

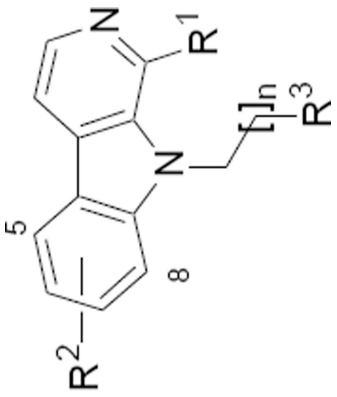

Cmpd	R^1	R^2	R^3	n	IC_{50} (μM)	
					Haspin	DYRK2
41	Me	7-OMe	NMe_2	3	0.47	> 10
42	CF_3	7-OMe	NH_2	3	0.10	15
43	CF_3	7-OH	NH_2	3	0.22	8.5